Flexoelectric Effect on Image Flickering of Fringe Field Switching LCDs

Haiwei Chen,[1] Fenglin Peng,[1] Minggang Hu,[1,2] and Shin-Tson Wu[1]

[1]College of Optics and Photonics, University of Central Florida, Orlando, Florida 32816, USA

[2] Xi'an Modern Chemistry Research Institute, Xi'an 710065, China

Abstract

We investigated the flexoelectric effect of a fringe field switching liquid crystal (LC) cell and characterized the resultant image flicker with different LC mixtures and frame rates. Incorporating with human eye perception of 10 observers, we found that LC mixtures with a dielectric anisotropy smaller than ~7 lead to unnoticeable image flicker at 60 frames per second. The obtained flicker sensitivity line serves as important guidelines for optimizing LC materials and display devices.

Keywords

Fringe field switching (FFS); Image flicker; Flexoelectric effect.

1. Introduction

Image flickering is an important issue as it affects the visual quality of a display device [1-3]. Several factors can cause image flickering, e.g. TFT leakage current and inadequate voltage holding ratio, but the dominant factors are flexoelectric effect (FEE) of the LC and human eye perception. Until now, there are only few studies on this effect in FFS LCDs, and most of previous reports concentrate on the observation and confirmation rather than understanding the detailed physical mechanisms. Thus, a systematic study to understand the mechanisms, quantify the effect, and then find solutions is urgently needed.

In this paper, we systematically investigate the FEE of FFS cell. Its origin can be described by the Gibbs free energy. We evaluate the image flicker of FFS cells with different | $\Delta\varepsilon$ | LC materials and different frame rates. Our experimental results indicate that keeping $\Delta\varepsilon \leq 7.2$ would suppress the flicker to unnoticeable level at 60 frame per second (fps). Incorporating with human eye perception of 10 observes, we obtain a flicker sensitivity line for FFS cell, which serves as important guidelines for optimizing LC materials and display devices.

2. Flexoelectric Effect of FFS LC Cell

FEE was first discovered and analysed by Meyer [4] and experimentally observed by Schmidt et al [5]. The FEE induced polarization could be described by:

$$\vec{P}_f = e_{11}\vec{n}(\nabla\cdot\vec{n}) + e_{33}(\nabla\times\vec{n})\times\vec{n}, \quad (1)$$

where e_{11} and e_{33} are flexoelectric coefficients, and $\vec{n}$ is the unit vector of the LC orientation. From Eq. (1), e_{11} and e_{33} are the two dominant factors governing the splay and bend deformations. Some methods for measuring e_{11} and e_{33} have been developed, although they are not simple [6-9]. In general, FEE is strong in a system whose molecules possess a large shape polarity as well as a large permanent dipole moment, which means there is a correlation between flexoelectric coefficients and dielectric anisotropy [4, 6].

In a FFS cell, the electric field is strong and not uniform in both lateral and longitudinal directions [10, 11]. Thus, the rod-like LCs are splayed and bent, which in turn causes a non-negligible flexoelectric polarization. Thus, the total Gibbs free energy consists of three terms: elastic, dielectric, and flexoelectric [12]:

$$F_{Elastic} = \frac{1}{2}K_{11}[\nabla\cdot\vec{n}]^2 + \frac{1}{2}K_{22}[\vec{n}\cdot(\nabla\times\vec{n})]^2 + \frac{1}{2}K_{33}[\vec{n}\times(\nabla\cdot\vec{n})]^2, \quad (2)$$

$$F_{Dielectric} = -\frac{1}{2}\varepsilon_0\Delta\varepsilon[\vec{n}\cdot\vec{E}]^2, \quad (3)$$

$$F_{flexo} = -[e_{11}\vec{n}(\nabla\cdot\vec{n}) + e_{33}(\nabla\times\vec{n})\times\vec{n}]\cdot\vec{E}, \quad (4)$$

$$F = F_{Elastic} + F_{Dielectric} + F_{Flexo}, \quad (5)$$

where $F_{Elastic}$ is the Frank elastic free energy density, $F_{Dielectric}$ is free energy associated with dielectric coupling, F_{Flexo} is the free energy contributed from flexoelectricity, K_{11}, K_{22}, and K_{33} are the splay, twist, and bend elastic constants.

From Eq. (4), the flexoelectric polarization is dependent on the polarity of the electric field. In a TFT-LCD, both positive and negative voltage frames are alternating in order to keep zero DC voltage. When the applied electric field is reversed (e.g. from positive to negative frame, or vice versa), from Eq. (4) the flexoelectric polarizations will be against the new electric field, leading to increased free energy density of the system. To lower the free energy density, the LC molecules will reorient slightly to form another stable configuration. During this polarity transition, the transmittance will change accordingly. When the electric field restores back, another optical transition occurs. Thus image flickers will arise with fluctuating transmittance when the polarity of electric field is altered regularly, as shown in Fig. 1(a) [1, 2].

Another evidence of FEE in a FFS cell is the difference of spatial transmittance between positive and negative voltage frames, as depicted in Fig. 1(b) [2, 13]. In the positive frame, the minimum transmittance occurs on the top of patterned electrodes, but it shifts to the middle of electrode gaps during negative frame. This clearly confirms the dynamic transition of LC director distributions caused by the flexoelectric polarization.

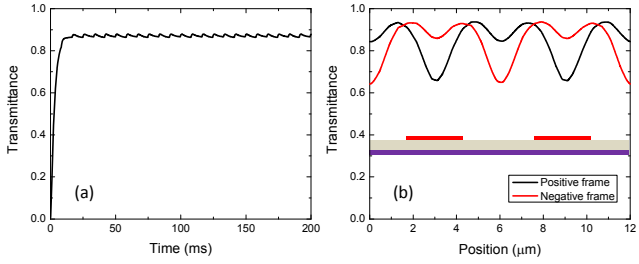

Fig. 1. (a) Simulated dynamic transmittance for alternating electric fields. (b) Simulated spatial transmittance distribution of positive and negative voltage frames. LC: $\Delta\varepsilon$ = 7.2, e_{11} = 15 pC/m, and e_{33} = 15 pC/m.

3. Experimental Results

In experiment, we investigate FEE from different influencing factors, including driving frequency, dielectric anisotropy, viscosity, and human eye sensitivity. A FFS cell with electrode width w = 3 μm, electrode gap l = 4 μm, and cell gap d = 3.5 μm

 ISSN 0097-966X/16/4701-0274-$1.00 © 2016 SID

was employed. Also, 5 different LCs were chosen to investigate the FEE, and their physical properties are listed in Table 1. Here, we define a flicker parameter as $F = \Delta T/T = (T_{max}\text{-}T_{min})/T_{ave}$ to quantify the transmittance change during frame inversion.

Table 1. Physical properties for different materials (T = 23 °C, λ = 550 nm, and f = 1 kHz.)

	$\varepsilon_{//}$	$\varepsilon_{\perp}$	$\Delta\varepsilon$	Δn	γ_1 (mPas)	T_c (°C)
MLC-6686	14.5	4.5	10.0	0.098	102.0	71.0
UCF-M1	10.8	3.6	7.2	0.099	58.1	77.9
UCF-M2	7.3	2.9	4.4	0.100	50.4	80.1
UCF-M3	6.2	2.7	3.5	0.103	45.1	77.9
ZOC-7003	3.6	8.0	-4.4	0.103	101.0	79.0

Fig. 2(a) shows the measured voltage-transmittance (VT) curves for two LC mixtures with different dielectric anisotropies ($\Delta\varepsilon$ = 10 and $\Delta\varepsilon$ = 4.4). With a smaller $\Delta\varepsilon$, both on-state voltage and peak transmittance increase [14]. Next, we investigated the voltage-dependent image flicker for both materials, as shown in Fig. 2(b). They exhibit a similar trend: as the operation voltage increases, the image flicker decreases first and then climbs up. In the low grey-level region, although the image flicker (quantified by the F-value) seems large (because of small denominator), the actual ΔT is relatively small. As a result, the flicker is hardly noticeable. In the middle grey-level region, T increases more rapidly than ΔT, resulting in a decreased F-value. However, this condition is reversed in the high grey-level region. Thus, in the following sections, we will evaluate image flicker at the on-state voltage, i.e. peak transmittance.

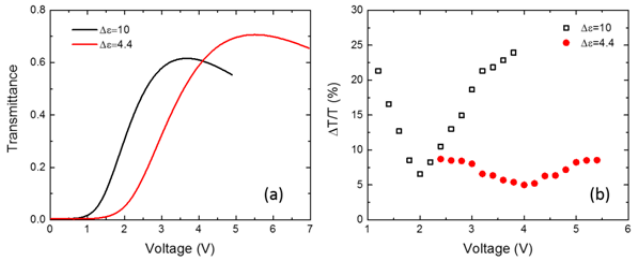

Fig. 2. Measured (a) VT curves and (b) image flicker of two LC mixtures with $\Delta\varepsilon$ = 10 and $\Delta\varepsilon$ = 4.4 (Table 1). FFS cell parameters: electrode width = 3 μm, electrode gap = 4 μm, and cell gap = 3.5 μm. λ = 633 nm.

3.1 Frequency effect

For mobile displays, 60 frames per second (fps) is the standard driving frequency. A lower frame rate helps reduce power consumption, but the flicker gets worse [1, 2]. Thus, image flicker caused by FEE is closely related to the driving frequency. Figure 3 shows the relation between flicker and frequencies. Clearly, as driving frequency decreases from 960 fps to 4 fps, image flicker gradually increases from 5% to 23%. The explanation is as follows: for a higher frame rate, each frame has a shorter duration, which is insufficient to stabilize the LC reorientation. Thus, the dynamic transmittance profile is like a pulse. The higher the frequency, the shorter each frame is, and then the smaller the transmittance difference. On the contrary, as frame rate decreases, each frame is long enough to allow the LC directors to complete the transition. Further decreasing frame rate causes flickering to saturate, as Fig. 3(e) depicts.

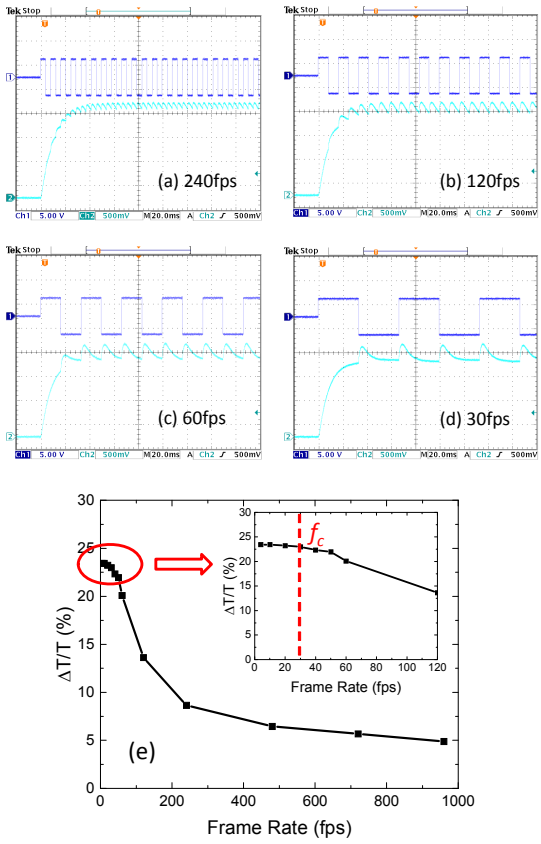

Fig. 3. (a) – (d) Dynamic transmittance at different frame rates. (e) Relation between image flicker and frame rate. (LC: MLC-6686 with $\Delta\varepsilon$ = 10 and λ = 633 nm)

3.2 Dielectric anisotropy effect

Next, we chose five LC mixtures (four positive and one negative) to investigate how the dielectric anisotropy influences the FEE of a FFS cell. The measured results are shown in Fig. 4. As $\Delta\varepsilon$ decreases from 10 to 3.5, the dynamic transmittance variation gets smaller, resulting in a suppressed image flicker. Meanwhile, when a LC mixture with negative $\Delta\varepsilon$ is employed (Fig. 4(e)), the transmittance changes more smoothly, which in turn leading to a negligible image flicker. These results are consistent with previous reports, where n-FFS mode exhibits unnoticeable image flickering [15, 16].

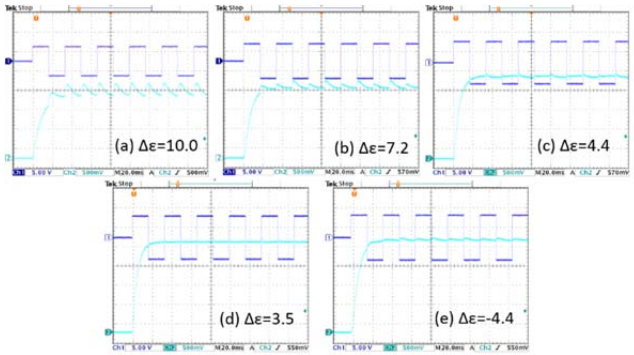

Fig. 4. (a) – (e) Dynamic transmittance for LC mixtures with different dielectric anisotropies. (Frame rate: 60 fps)

Figure 5 summarizes the F value for each LC mixture. Clearly, the image flicker keeps decreasing from 20% to 6% when $\Delta\varepsilon$ decreases from 10 to 3.5. More amazingly, the F value drops to 3.5% with $\Delta\varepsilon = -4.4$. From Eq. (1), the flexoelectric polarization is governed by two factors: e_{11} and e_{33}, and spatial derivatives of the LC directors $\vec{n}$, or namely the deformations of LC molecules. For a positive LC, larger $\Delta\varepsilon$ means larger dipole moment and larger shape polarity, thus a larger flexoelectric coefficient is expected. What's more, a large tilt deformation will be induced if the LC has a large $\Delta\varepsilon$, which in turn amplifies the flexoelectric polarization [14]. Therefore, the image flicker increases with increasing $\Delta\varepsilon$. For a negative $\Delta\varepsilon$ material, the LC molecules are more uniformly distributed [15, 16], leading to a much smaller flickering.

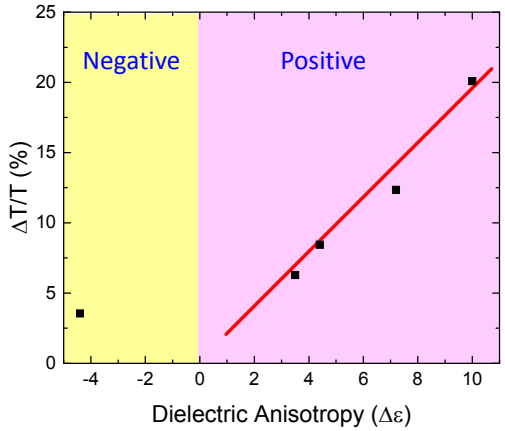

Fig. 5. Relation between image flicker and dielectric anisotropy. (Frame rate: 60 fps)

3.3 Viscosity effect

In Fig. 3(e), there exists a critical frequency (f_c); below which the image flicker does not change any more. This is because the LC directors have enough time to relax and the resultant transmittance saturates, as Fig. 3(d) shows. Obviously, this critical frequency depends on the speed of LC reorientation. If the LC has faster response time, a shorter time is needed to complete the transition between different frames. Thus, image flicker will saturate at higher frequency, as depicted in Fig. 6. For a low viscosity LC mixture, say $\gamma_1 = 45$ mPas, the critical frame rate is as high as 240 fps. It indicates the image flicker would remain the same as long as the frame rate is slower than 240 fps. Meanwhile, low flicker is expected since low viscosity and low dielectric anisotropy are usually correlated [17].

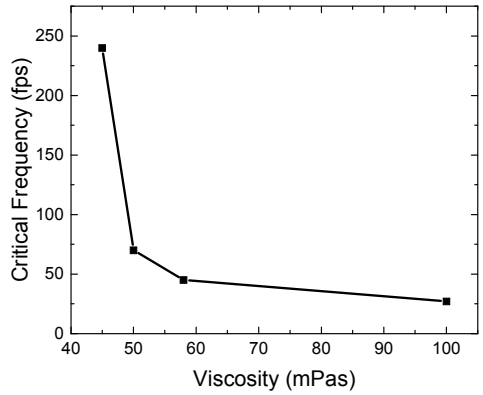

Fig. 6. Measured critical frame rate vs. LC rotational viscosity.

3.4 Flicker sensitivity

Until now, we use the parameter F to quantitatively compare the image flicker for different materials at different frame rates. However, we have not yet considered the human eye sensitivity. In reality, we need to figure out at which level the flicker would be detectable by the human eye. This could be characterized by the flicker sensitivity, which is a concept in the psychophysics of vision [18, 19]. It is defined as the modulation depth at which an intermittent light stimulus appears to be completely steady to the average human observer when measured at a series of fixed frequencies.

Several parameters affect the ability to detect flicker, such as frame rate, modulation depth, illumination intensity, wavelength (or wavelength range) of the illumination, the position on the retina at which the stimulation occurs, the degree of light or dark adaptation, and the physiological factors such as age and fatigue [20, 21]. In our experiment, we invited 7 males and 3 females (age between 25 and 30) as observers. The employed light source is Pocker-Vue CL-5000P with cold cathode tube, driven by DC current in order to eliminate the blinking of backlight. Also, the experiment was conducted under dimmed ambient light. Results are shown in Fig. 7. As expected, as the frame rate increases, the threshold modulation depth increases in order to notice flickering. This trend is consistent to previous finding for flicker perception [13, 18-19].

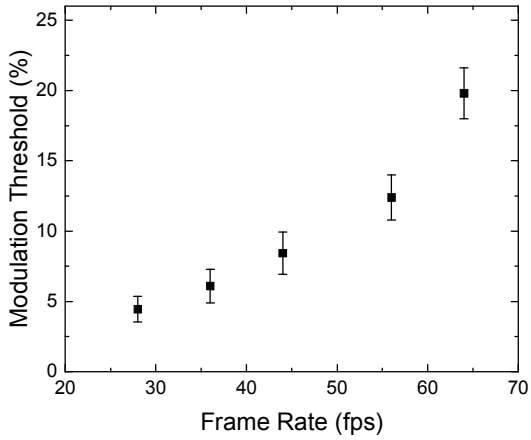

Fig. 7. Relation between modulation threshold and frame rate.

4. Discussion

Detecting image flicker is quite subjective; it depends on human eye's perception. Therefore, the absolute value $F = \Delta T/T$ alone is difficult to quantify image flicker. Instead, the flicker sensitivity line representing the threshold (heavy green line, Fig. 8) is more meaningful in reality. Above this line, the flicker is noticeable, leading to degraded image quality and eye strain. Below this line, the flicker is unnoticeable.

This flicker sensitivity line serves as important guidelines for optimizing LC materials and display devices. For example, if we want to drive an LCD at 60 fps, then we should keep $\Delta\varepsilon \leq 7.2$. On the other hand, if an LC with $\Delta\varepsilon = 4.4$ is employed, the driving frequency should be higher than 40 fps in order to suppress flicker to invisible level. From Fig. 8, the yellow region means image flickering is unnoticeable to the human eye.

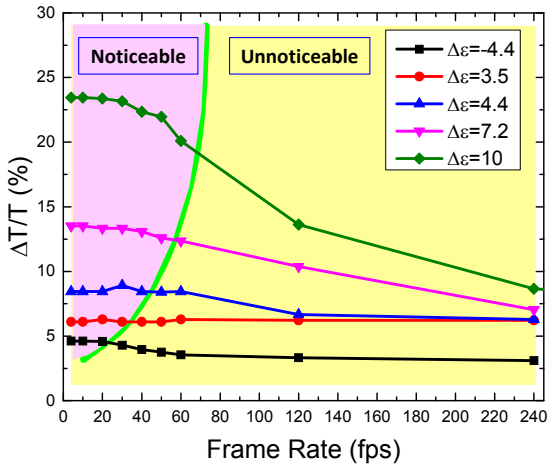

Fig. 8. Frame rate dependent image flicker for LC mixtures with different dielectric anisotropies. The heavy green line represents the flicker sensitivity boundary.

As discussed above, the flicker detection is governed by several factors. Thus in real applications, the flicker sensitivity line obtained here could vary slightly for different purposes and different device configurations. For example, the strength and spectrum of the backlight, the electrode structure of FFS cell, and the driving frequency of TFT will play important roles in flicker perception. What's more, the expected consumer groups should also be taken into consideration, since the physiological factors such as age and fatigue will take effect as well. With so many variables, however, our flicker sensitivity line still serves as an important guideline for further optimizations. Meanwhile, low $\Delta\varepsilon$ LC mixtures exhibit smaller image flicker; this tendency should be consistent despite of the device configurations.

5. Conclusion

We have analysed the flexoelectric effect in FFS cell thoroughly, and the image flickers are measured and compared with different materials at different frame rates. By comparison, we found that LC mixtures with a small but positive $\Delta\varepsilon$ help to suppress the flexoelectric effect, and image flicker with $\Delta\varepsilon \leq 7.2$ is unnoticeable at 60 fps. Besides, flicker sensitivity line for FFS cell is obtained, which offers the guidance for optimizing LC materials and display devices. This discovery will make a great impact to mobile displays, especially for the elimination of image flicker using a positive $\Delta\varepsilon$ LC mixture.

6. References

[1] K. C. Chu, C. W. Huang, R. F. Lin, C. H. Tsai, J. N. Yeh, S. Y. Su, C. J. Ou, S. C. Fan Jiang, and W. C. Tsai, "A method for analyzing the eye strain in fringe-field-switching LCD under low-frequency driving," SID Int. Symp. Digest Tech. Pap. **45**, 308–311 (2014).

[2] I. H. Jeong, I. W. Jang, D. H. Kim, J. S. Han, B. Y. Kumar, S. H. Lee, S. H. Ahn, S. H. Cho, and C. Yi, "Investigation on flexoelectric effect in the fringe field switching mode," SID Int. Symp. Digest Tech. Pap. **44**, 1368–1371 (2013).

[3] R. Hatsumi, S. Fukai, Y. Kubota, A. Yamashita, M. Jikumaru, H. Baba, K. Moriya, D. Kubota, K. Kusunoki, Y. Hirakata, J. Koyama, S. Yamazaki, Y. Chubachi, and C. Fujiwara, "FFS-mode OS-LCD for reducing eye strain," J. Soc. Inf. Display **21**, 442–450 (2013).

[4] R. B. Meyer, "Piezoelectric effects in liquid crystals," Phys. Rev. Lett. **22**, 918-921 (1969).

[5] D. Schmidt, M. Schadt, and W. Helfrich, "Liquid-crystalline curvature electricity: the bending mode of MBBA," Zeitschrift für Naturforschung A **27**, 277-280 (1972).

[6] C. Kischka, S. J. Elston, and E. P. Raynes, "Measurement of the sum (e1+e3) of the flexoelectric coefficients e1 and e3 of nematic liquid crystals using a hybrid aligned nematic (HAN) cell," Mol. Cryst. Liq. Cryst. **494**, 93-100 (2008).

[7] F. Castles, S. C. Green, D. J. Gardiner, S. M. Morris, and H. J. Coles, "Flexoelectric coefficient measurements in the nematic liquid crystal phase of 5CB," AIP Advances **2**, 022137 (2012).

[8] R. A. Ewings, C. Kischka, L. A. Parry-Jones, and S. J. Elston, "Measurement of the difference in flexoelectric coefficients of nematic liquid crystals using a twisted nematic geometry," Phys. Rev. E **73**, 011713 (2006).

[9] T. Takahashi, S. Hashidate, H. Nishijou, M. Usui, M. Kimura, and T. Akahane, "Novel measurement method for flexoelectric coefficients of nematic liquid crystals," Jpn. J. Appl. Phys. **37**, 1865-1869 (1998).

[10] S. H. Lee, S. L. Lee, and H. Y. Kim, "Electro-optic characteristics and switching principle of a nematic liquid crystal cell controlled by fringe-field switching," Appl. Phys. Lett. **73**, 2881-2883 (1998).

[11] D. H. Kim, Y. J. Lim, D. E. Kim, H. Ren, S. H. Ahn, and S. H. Lee, "Past, present, and future of fringe-field switching liquid crystal display, " J. Infor. Display, **15**(2), 99-106 (2014).

[12] L. M. Blinov and V. G. Chigrinov. *Electrooptic Effects in Liquid Crystal Materials*. Springer-Verlag; 1994.

[13] J. W. Kim, T. H. Choi, T. H. Yoon TH, E. J. Choi, and J. H. Lee, "Elimination of image flicker in fringe-field switching liquid crystal display driven with low frequency electric field," Opt. Express **22**, 30586-30591 (2014).

[14] H. Chen, F. Peng, Z. Luo, D. Xu, S. T. Wu, M. C. Li, S. L. Lee, and W. C. Tsai, "High performance liquid crystal displays with a low dielectric constant material," Opt. Mater. Express **4**, 2262-2273 (2014).

[15] Y. Chen, Z. Luo, F. Peng, and S. T. Wu, "Fringe-field switching with a negative dielectric anisotropy liquid crystal," J. Display Technol. **9**, 74-77 (2013).

[16] H. Chen, Y. Gao, and S. T. Wu, "n-FFS vs. p-FFS: who wins?" SID Int. Symp. Digest Tech. Pap. **46**, 735–738 (2015).

[17] H. Chen, M. Hu, F. Peng, J. Li, Z. An, and S. T. Wu, "Ultra-low viscosity liquid crystals," Opt. Mater. Express **5**, 655-660 (2015).

[18] C. W. Tyler, "Analysis of normal flicker sensitivity and its variability in the visuogram test," Investigative Ophthalmology & Visual Science **32**, 2552-2560 (1991).

[19] S. Shady, D. I. A. MacLeod, and H. S. Fisher, "Adaptation from invisible flicker," PNAS **101**, 5170-5173 (2004).

[20] G. W. Brundrett, E. Eng, and M. Mech, "Human sensitivity to flicker," Lighting and Research Technology **6**, 127-143 (1974).

[21] S. Wu, S. A. Burns, and A. E. Elsner, "Effects of flicker adaptation and temporal gain control on the flicker ERG," Vision Res. **35**, 2943-2953 (1995).